Photogrammetrische Woche 1985
Institut für Photogrammetrie
Schriftenreihe, Heft 11, 1986

ON AUTOMATIC MEASUREMENT OF DIGITAL SURFACE MODELS

W. Förstner, Stuttgart

0. Introduction

One of the most important features for the description of an object is the geometric form of its surface. There are a variety of methods available for the measurement of surface forms. They differ from one another in many aspects, in particular according to the size of the objects, the relative accuracy and the physical measuring principles. Of special interest amongst these are the non-tactile procedures due to their flexibility. Photogrammetric methods present themselves above all as an economic alternative in many areas of measurement techniques (cf. Wrobel, 1981). Up to now photogrammetric methods have not generally prevailed in close range applications. The reason for this might well be the film development, where the time span between the taking of the photograph and the result is too long for some applications. The television technique and later the video technique for the recording of photographs have fundamentally altered the situation: the photogrammetric measurement of surfaces in real time is, in principle, becoming possible. The existing operational or experimental, automatic and semi-automatic systems admittedly necessitate in contrast to the visual system of the human being a very long time; it can, however, be clearly seen that methods will be available in the near future which under not too restrictive conditions will be able to determine surfaces economically and with an accuracy comparable to that of analogue methods.

There already exist a series of general articles for automatic stereo measurement. Konecny and Pape (1981) and Case (1981) describe instruments, algorithms and methods for stereo correlation, as implemented in the field of photogrammetry. Baker (1981) and Barnard and Fischler (1982) give a summary of the methods existing in the USA for automatic stereo measurement. In addition to this Barnard and Fischler discuss in detail the individual steps within such methods, in particular the parameters essential for each step. One can accordingly distinguish the following sequence of steps within the method:

1) taking of the photograph
2) calibration and orientation
3) feature selection
4) matching the features
5) distance or depth determination
6) interpolation.

Steps 1, 2, 5 and 6 are familiar as standard photogrammetric tasks. The selection of distinct features (step 3) and the matching process (step 4) take place at photogrammetric instruments, generally performed by an operator. The automization of these steps is discussed for example by Förstner (1985) for image pairs and by Kories (1985) for image sequences.

This contribution deals with specific aspects for automatic surface measurement from pairs of photographs. In particular these are the geometry of the photograph and of the surface (section 2) the judgement or selection of surface textures (section 3) and the representation of the surface by the measurement elements (section 4). An attempt is made to illustrate the influence of necessary decision in individual cases on the method steps and thus also the influence on their mutual dependence.

1. Model assumptions

1.1 Models for surface description

The difficulty of reconstructing an object surface depends essentially upon its complexity. According to Hobrough (1978) five degrees of complexity can be discerned (cf. Fig. 1-1). The transition from class a) to b) can be achieved by an expansion of the mathematical mode. Class c) can be dealt with by reduction of each of the observed image windows. The treatment of profiles or areas of class d) presupposes, strictly speaking, the automatic localization of the discontinuities, can however still be approximated by piecewise linear profiles or patches. Class e) profiles presuppose firstly that the area sections nearer to the observer - at least piecewise - are transparent and secondly that the method is able to process several heights per point. Although this class of areas can, circumstances permitting, be approximated by piecewise linear patches - alternately on one or the other of the surfaces - and although the solubility has been experimentally demonstrated (Grimson 1981), we want to exclude in the following surfaces of class e).

Surfaces can then be regarded as piecewise smooth functions. The edges of the surface sections do not need to be closed. The boundaries can be jumps in the height, in the slope or also in the curvature (cf. Binford 1981).

Apart from being dependent on the macro structure, i. e. the geometry, the reconstructability of the surface also depends upon its micro structure, i. e. its texture. Thereby are summarily meant all the in detail generally unknown radiometric characteristics of the surface. They decide how the object is represented in the photograph in dependence upon the lighting, the geometry and the features of the sensor.

Fig. 1-1 Degrees of complexity for surfaces (according to Hobrough 1978)

a) plane, horizontal
b) plane, sloping
c) continuous
d) not continuous
e) multiple

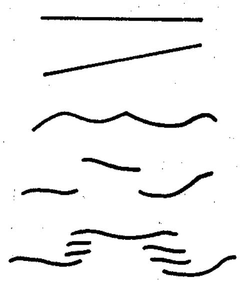

For the reconstruction from photographs one generally supposes that the surface is matt, i. e. that surface points appear equally bright from all sides or that the surface distributes the light equally in all directions. These models are for example used to reconstruct the surface - with certain restrictions - from the shading in one or several photographs (Inverse Shading, Woodham 1981, Ikeuchi/Horn 1981; Photometric Stereo, Woodham 1980). They also implicitly form the basis of all methods of correspondence which base themselves on the brightness' distribution as feature of points, as e. g. the classical method of correlation. The justified criticism of these models leads to the fact that often not the distribution of the brightness itself but the transitions of areas of equal brightness, i. e. grey value edges, are used as features for matching. The disturbing influence of local and also temporal (cf. Wiesel 1981) changes of the reflection behaviour on the correspondence is hereby extensively eliminated (cf. sect. 2). Above all the demands on the radiometric calibration are hereby rendered less acute (cf. Binford 1981, Gülch 1985).

1.2 Models for projection

The geometric projection for photographs with area sensors is sufficiently described by the central perspective. With amateur or partially metric cameras a suitable geometric calibration serves to reduce the geometric projection properties to those of the central perspective. The parameters of the exterior, at least of the relative orientation of the photographs are assumed in the following to be known.

For the radiometric projection the decisive parameters are the resolution, the distance between the pixels and the sensitivity of the sensor elements. Apart from the texture of the object they also determine the accuracy of the correspondence (cf. Förstner 1985). The resolution can be represented in detail by the modulation transfer function of the light path from the object to the sensor element. We want to suppose that these parameters are known and adapted to each other.

2. Geometry of photograph and surface

The geometry of the photograph and of the surface determines the efficiency of the whole procedure. In particular the correspondence algorithm must be able to allow for geometric distortions caused by the relative slope of the surface to the photograph coordinate system. Conversely the surface slope derivable from the distortions should go into the concluding interpolation. The use of epipolar geometry and suitable transformations between the various coordinate systems is of decisive importance for the efficiency and it is for this reason that we will discuss it first of all.

2.1 Epipolar Geometry

After the relative orientation of the photographs the rays of corresponding image points intersect at the object point, if one disregards minor photographic errors. Object points, image points and projection centres lie on one plane, the epipolar plane (cf. Fig. 2-1).

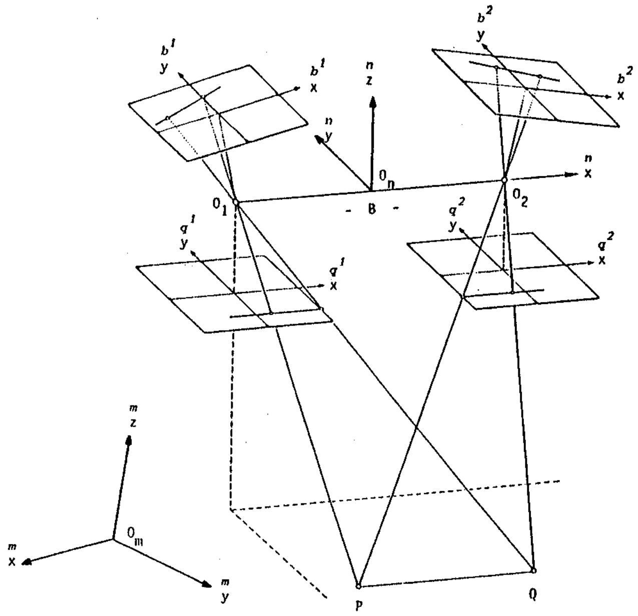

Fig 2-1 Normal images according to Kreiling (1978)

b^1, b^2 image coordinate system
p^1, p^2 normal image coordinate system
n natural model coordinate system
m model system

The advantage of this geometric condition for the automatic correspondence of image windows lies in the fact that the otherwise area type search space for the correspondence, as it is the case with the relative orientation, is reduced to a line, namely the epipolar line assigned to the point (cf. Helava 1972). Not only the computation time is considerably lessened by this. More importantly changes in the grey value running diagonal to the epipolar lines, say, grey value edges, can be used for correspondence which otherwise would not allow a transfer, say, along the edge. The differential perspective projection is restricted to three parameters, which correspond to the height and the two surface slopes. In order to simplify the representation or the calculations, too, one proceeds to a pair of normal images (see Fig. 2-1, Kreiling 1978). It is achieved by projecting the images with general orientation in space onto a plane parallel to the base. The position of this plane is in principle arbitrary, it is, however, useful to choose the distance from the base equal to the focal length and the orientation of the plane symmetrical to the two images. The epipolar lines lie parallel to one another in the normal photographs. In addition, the perspective relations between the image and object coordinates are reduced to simple relations, if one refers to the natural coordinate system n of the relatively oriented image pair. Epipolar geometry is used by nearly all correspondence procedures for surface determination.

2.2 Homogeneous Coordinates and Coordinate Transformation

A large number of different coordinate systems occur with the practical realisation, amongst which the most advantageous according to the respective problem is selected for the representation or calculation. Apart from shifts, rotations and affinities, also perspective transformations occur. Fig. 2-2 shows the relations between the coordinate systems in the form of a commutative diagram, such as they can occur with image correspondence when using an analytical plotter. In detail there are the following systems in

- *b(2)* image (see Fig. 2-1)
- *c(2)* photo carriage
- *s(2)* sensor, CCD camera
- *t(2)* sensor window
- *t(2)* projected normal image
- *q(2)* normal image window
- *f(2)* surface point (x-axis on the epipolar plane)
- *n(3)* normal model (see Fig. 2-1)
- *m(3)* model, object (see Fig. 2-1)

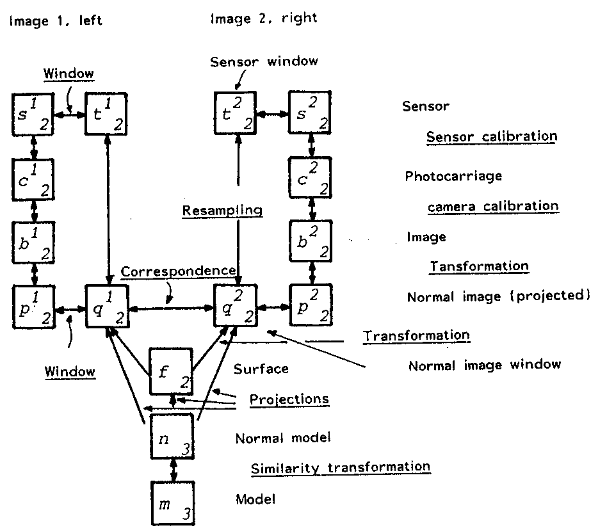

Fig. 2-2 Coordinate systems and transformations for image correspondence with an analytical plotter (commutative diagram)

The bracketed figures specify the dimensions of the respective system. Systems related to images are signified by the image number (1, 2...) (cf Fig. 2-1). The transformations between the individual coordinate systems result partially from calibrations, from the relative orientation or from the correspondence algorithm. E. g. from the geometrical sensor calibrations (cf. Gülch 1985) one obtains the transformations:

$$T_s^c : \begin{pmatrix} x \\ y \end{pmatrix}^c = T_s^c \left\{ \begin{pmatrix} x \\ y \end{pmatrix}^s \right\} = A_s^c \begin{pmatrix} x \\ y \end{pmatrix}^s + a_s^c \qquad (2\text{-}1)$$

If the correspondence relates to the windows q^1 and q^1 from the normal images the transformation T_t^q is required for the interpolation of the grey values from the sensor windows t^1 and t^2. It is not directly available, but can be obtained from known transformations:

$$T_t^q = T_p^q \; T_b^p \; T_c^b \; T_s^c \; T_t^s \qquad (2\text{-}2)$$

and apart from the two transformations T_p^q and T_s^t for the formation of the windows contains the calibration transformations T_s^c and T_c^b of the CCD and of the photogrammetric camera and the projective transformation T_b^p from the image into the normal image. If T is regular, then $T_h^q = (T_q^h)^{-1}$.

The projective transformations cannot be represented in the form of eqn. (2-1), then one could obtain compounded transformations by matrix multiplication. With image windows of size 5 x 5 mm² a linearization would lead to inadmissable errors. A concatenation with matrix multiplication can, however, be achieved by the application of homogenous coordinates. They are standardly used in the field of CAD and are also commonly used in robotics (cf. Haralick 1980, Ballard/Brown 1982).

In principle the coordinate vector $(x, y)'$ or $(x, y, z)'$ is expanded for this purpose by one coordinate, which corresponds to a scale factor. In this way one obtains the vectors $(u, v, t)'$ or $(u, v, w, t)'$. The coordinates x, y, and perhaps z can be caluculated from the homogenous coordinates u, v, t and perhaps also w:

$$x = \frac{u}{t}, \quad y = \frac{v}{t}, \quad z = \frac{w}{t} \qquad (2\text{-}3)$$

A common scale within homogenous coordiantes does not alter the related 3D-coordinates. Homogeneous coordinates are redundant.

The perspective projection with the centre of projection at the origin and the image plane at the level $z = c$

$$x' = c\frac{x}{z}, \; y' = c\frac{y}{t}, \; z' = c \qquad (2\text{-}4a)$$

can be written in homogenous coordinates as the matrix product

$$\begin{pmatrix} u' \\ v' \\ w' \\ t' \end{pmatrix} = \begin{pmatrix} 1 & 0 & 0 & 0 \\ 0 & 1 & 0 & 0 \\ 0 & 0 & 1 & 0 \\ 0 & 0 & \frac{1}{c} & 0 \end{pmatrix} \begin{pmatrix} u \\ v \\ w \\ 1 \end{pmatrix} \quad \text{or} \quad \begin{pmatrix} u' \\ v' \\ t' \end{pmatrix} = \begin{pmatrix} 1 & 0 & 0 & 0 \\ 0 & 1 & 0 & 0 \\ 0 & 0 & \frac{1}{c} & 0 \end{pmatrix} \begin{pmatrix} u \\ v \\ w \\ 1 \end{pmatrix} \qquad (2\text{-}4b)$$

as can be verified by matrix multiplication. The form 2-4b shows that a reduction in dimension can also be clearly represented. As was to be expected, the inverse transforamtion does not exist since the transformation matrix is singular. A projective transformation such as T_p^b has the form

$$\begin{pmatrix} u \\ v \\ t \end{pmatrix} = \begin{pmatrix} a & b & c \\ d & e & f \\ g & h & i \end{pmatrix}_p^b \begin{pmatrix} u \\ v \\ 1 \end{pmatrix}^p \qquad (2\text{-}5a)$$

and corresponds to the known equations

$$x^b = \frac{a\,x^p + b\,y^p + c}{g\,x^p + h\,y^p + i} \qquad y^b = \frac{d\,x^p + e\,y^p + f}{g\,x^p + h\,y^p + i} \qquad (2\text{-}5b)$$

whereby the marking of the coefficients with respect to the chosen coordinate system was surpressed.

The elements of the general transformation matrix for four homogenous coordinates

$$T = \left(\begin{array}{ccc|c} M_x & & S & V_x \\ & M_y & & V_y \\ S & & M_z & V_z \\ \hline P_x & P_y & P_z & M \end{array}\right) \qquad (2\text{-}6)$$

can be directly interpreted as individual scales M_x, M_y, M_z, as a general scale (M), as shifts (V_x, V_y, V_z) as shears or as perspectives (P_x, P_y, P_z). For a pure similarity transformation the upper left 3 x 3 matrix contains the rotation matrix, the elements P_k are zero.

In case of practical application a large part of the transformation remains unchanged as it is only dependent upon the calibration and the relative orientation. The transformation compounded from these transformations, therefore, only needs to be calculated once. The different transformations for each point, which are caused by the different sensor positions and the varying positions and orientation of the observed surface area, can be added to the left or the right of the constant transformation. Changes in calibration can easily be incorporated. Altogether an efficient instrumentation for the representation and calculation of geometric relations thus is available, which can be adapted to each individual situation. In the following, however, we nevertheless refer to the classical representation as it is clearer in the case of only two or three coordinate systems.

2.3 Geometric distortions of the projection

A decisive factor when selecting a method for automatic surface measurement form images is which distortions in the projection have to be expected. The distortions between the photographs can be quantatively described by the scale factor m and the shearing s of the two small image windows which are related to the normal image system q. In principle occlusions and thus values for the scale smaller than or equal to zero can occur even with smooth surfaces, for example at the contours of the surfaces. Even if one avoids occlusions when taking the photograph, considerable differences in scale and relative shearings can occur between the photographs.

If one starts from a normal image pair, one obtains from the projection relations $x_1 = c\,(X+B/2)/Z$, $x_2 = c\,(X-B/2)/\,Z$ and $y_1 = y_2 = y = c\,Y/Z$ the following expressions for the scale factor m and the relative shear if one takes into consideration for m only the longitudinal slope $Z_X = \partial Z/\,\partial Z$ and for s only the lateral slope $Z_Y = \partial Y$

$$m = \frac{dx_2}{dx_1} = \frac{Z - (X-B/2)\; Z_X}{Z - (X+B/2)\; Z_X} \qquad (2\text{-}7)$$

$$s = \frac{dx_2 - dx_1}{dy} = \frac{B\; Z_Y}{Z - Y\; Z_Y} \qquad (2\text{-}8)$$

Here X, Y and Z are the object coordinates in the normal model (n), B the base length, (x_1, y_1) and (x_2, y_2) the coordinates in the left and right normal image respectively and Z_x and Z_y the longitudinal and lateral slope respectively in the normal model.

The most unfavourable scale factor is obtained with $X = B/2$ as (within the model):

$$\bar{m}(Z_X) = \frac{1}{1 - B/Z \; Z_X} \tag{2-9}$$

the most unfavourable shear with $Y = B$ as

$$\bar{s}(Z_Y) = \frac{B/Z \; Z_Y}{1 - B/Z \; Z_Y} = \bar{m}(Z_X) - 1 \tag{2-10}$$

The most unfavourable scale distortions for varying base-height ratios B/Z and slopes Z_X are compiled in Table 2-1.

		Z_X:					
B/Z	*Type*	*0.1*	*0.2*	*0.5*	*0.7*	*1.0*	*2.0*
1.1	*SWA*	*1.12*	*1.28*	*2.22*	*4.35*	-	-
0.6	*WA*	*1.06*	*1.14*	*1.43*	*1.72*	*2.50*	-
0.3	*NA*	*1.03*	*1.06*	*1.18*	*1.27*	*1.43*	*2.50*

Tab. 2-1 Scale distortions $\bar{m}$ according to Equ. 2-9 in dependence upon the base-height relation B/Z of current aerial photograph sensors and the terrain slope $Z_x = \tan\alpha$. The maximum shears as to be expected are smaller by 1.

When using a wide-angle camera ($B/Z = 0.6$) scale differences of up to 1 : 2.5 and shears of up to 1.5 can be expected for slopes of the surface of 45° ($Z_X = 1$). An angle of 73° between the images of the y-axis in the surface system (f) corresponds in the most disadvantageous case to a shear of 1.5. As surface slopes of this size can readily occur in close range applications, also, however, during the measurement of aerial photographs on steep slopes and house rooves, a correspondence method must be capable of processing such large distortions. Neglection of the distortions leads at the very least to a considerable reduction of the correspondence accuracy, if it does not make the correspondence fail. A correspondence method must, therefore, either have reliable approximations available for the distortions, such as by prediction from earlier measurements, or it must rely on features which are invariant against affine distortions (cf. sect. 4).

2.4 Measurement of Surface Slopes

Conversely one can derive the surface slope from the estimated values for the affine distortions. Let the general linear transformation (without taking the epipolar geometry into consideration) for the image windows be in differential form

$$dx_1 = a_{11}\, dx_2 + a_{12}\, dy_2 \tag{2-11a}$$

$$dy_1 = a_{21}\, dx_2 + a_{22}\, dy_2 \tag{2-11b}$$

If the x-axis of the photograph coordinate system approximately (± 30°) coincides with the epipolar line, the surface slopes can be derived from the coefficients a_{11} and a_{12} (eqn. 2-11a). since the two coefficients approximately correspond to scale and shearing.

$$Z_X = \frac{a_{11}\frac{\partial x_2}{\partial X} + a_{12}\frac{\partial y_2}{\partial X} - \frac{\partial x_1}{\partial X}}{a_{11}\frac{\partial x_2}{\partial Z} + a_{12}\frac{\partial x_2}{\partial Z} - \frac{\partial x_1}{\partial Z}} \qquad Z_Y = \frac{a_{11}\frac{\partial x_2}{\partial Y} + a_{12}\frac{\partial y_2}{\partial Y} - \frac{\partial x_1}{\partial Y}}{a_{11}\frac{\partial x_2}{\partial Z} + a_{12}\frac{\partial y_2}{\partial Z} - \frac{\partial x_1}{\partial Z}} \tag{2-12}$$

The partial deviations in eqn. 2-12 can be derived from the parameters of the exterior orientation (cf. Schwidefsky/Ackermann 1976).

With a good surface texture one can obtain the parameters a_{11} and a_{12} with an accuracy of approximately 0.02. The derived slope angles of the surface with respect to the object coordinate system then have a standard deviation of approximately 1-3°. The slopes measured in this way should be used for the interpolation of the surface.

2.5 Interpolation

The measured points resulting from the correspondence are generally not identical with the digital surface model. Even if they are planned to ly in a grid in general, individual points will be missing, because the texture does not permit a measurement. An interpolation is practically always necessary in order to arrive at a final surface model (see sect. 4 on the choice of point distribution).

Basically we have greatly varying information about the surface, which can be used for the interpolation

- surface points
- surface slopes
- lack of shading which suggest smoothness of the surface
- grey value edges which suggest possible object edges
- accuracy data about the measurements
- non-matched points which suggest occlusions
- contour lines
- a mathematical model for the surface form, e. g. planes, surfaces of the second order, general cones, symmetry axes, smoothness requirements etc..

There is presumably no method which uses all the named information for the derivation of the digital surface model.

According to the data used one can distinguish amongst other things the following approaches:

a) The surface is assumed to be smooth.
The smoothness of the surface can most easily be determined by its curvature. The second derivations of the surface can be summarized for each point P_{ij} in the Hessian matrix

$$H_{ij} = \begin{pmatrix} Z_{XX} & Z_{YY} \\ Z_{YX} & Z_{YY} \end{pmatrix} \qquad (2\text{-}13)$$

If one neglects the surface slope, the principle radii of curvature result from the values of the Hessian matrix: $r_a = 1/\lambda_a$. There now exist two measures for the total curvature of the surface which are both invariant against rotations of the coordinate system

$$L = \sum_{ij}\sum \left(\frac{1}{r_a} + \frac{1}{r_b}\right)^2 = \sum_{ij}\sum (Z_{XX} + Z_{YY})^2 = \sum_{ij}\sum (\nabla^2 Z)^2 = \sum_{ij}\sum (\mathrm{sp}\, H_{ij})^2 \qquad (2\text{-}14)$$

and

$$Q = \sum_{ij}\sum \left(\frac{1}{r_a^2} + \frac{1}{r_b^2}\right) = \sum_{ij}\sum Z_{XX}^2 + 2\, Z_{XY}^2 + Z_{YY}^2 = \sum_{ij}\sum \mathrm{sp}\,(H_{ij}^2) \qquad (2\text{-}15)$$

L is the Laplacian curvature, Q the so-called Quadratic Variation of the surface. All other rotation-invariant measurements for the curvature can be represented as the weighted sum of the two values.Theoretically and practically the Quadratic Variation has turned out to be superior for the purposes of interpolation, as is shown by the investigation of Grimson (1981).

Interpolation can be achieved by minimization of the weighted sum of the quadratic deviations $z_k - \hat{z}_k$ at the given points and of the Quadratic Variation:

$$\Phi_1(\hat{z}_k) = \sum_k (z_k - \hat{z}_k)^2 + \beta^2 \sum_{ij}\sum \mathrm{sp}\,(\hat{H}_{ij}^2) \rightarrow \min \qquad (2\text{-}16)$$

The factor β^2 weights the measured values against the smoothness requirement. The optimization problem can either be solved iteratively (Grimson 1981) or directly (such as by Ebner 1979).

b) The surface is assumed to be partially smooth.
In this case eqn. 2-16 is no longer suited for interpolation. However, by individual weighting of the curvatures one can remove the smoothness requirement at those places where grey value edges appear in the image, and hence one can presume that there is an object edge. In this way we obtain

$$\Phi_2(\hat{z}_k) = \sum_k (z_k - \hat{z}_k)^2 + \sum_{ij}\sum \beta_{ij}\, \mathrm{sp}\,(\hat{H}_{ij}^2) \rightarrow \min \qquad (2\text{-}17)$$

Eqn. (2-17) is related to the statement of Nagel (Nagel/Engkelmann 1984) who for image sequence analysis along the grey value edges weights down the smoothness requirement for the field of shifts according to the sharpness of the edges.

c) The accuracy of the measured values is taken into consideration.
The precision of the measured values is not used for the optimization problem eqns. 2-16 and 2-17. The consistency of the solution i. e. the fulfillment of the smoothness requirement by the measured values is likewise not used for the improvement of the interpolation.

Both is possible if one slightly modifies eqn. 2-17

$$\Phi_3(\hat{z}_k, \hat{\sigma}_{ij}) = \sum_k \frac{(z_k - \hat{z}_k)^2}{\sigma_k^2} + \sum_{ij} \frac{sp(\hat{H}_{ij}^2)}{\hat{\sigma}_{ij}^2} \rightarrow \min$$

On one hand the standard deviations σ_k of the measured values can then be taken into consideration, and on the other hand the standard deviations σ_{ij} of the curvatures at the grid points in dependence upon both the grey values (cf. Nagel) and also upon consistency of the solution, i. e. upon the curvatures after the estimation. The weights $\beta_{ij} = 1/\sigma_{ij}^2$ are then estimated in the sense of a variance estimation, or a robust estimation (cf. Li 1984), an automatic edge detection (see Fig. 2-2).

d) The measured slopes are used.

The implementation of the measured slopes z_x and z_y leads to a stabilization of the surface (cf Förstner 1983) and can be be realised by an additional term in eqn. 2-18:

$$\Phi_4(\hat{z}_k, \hat{\sigma}_{ij}) = \Phi_3(\hat{z}_k, \hat{\sigma}_{ij}) + \sum_i \{(z_{X,1} - \hat{z}_{X,1})^2 + (z_{Y,1} - \hat{z}_{Y,1})^2\}/\sigma_1^2 \rightarrow \min \qquad (2\text{-}19)$$

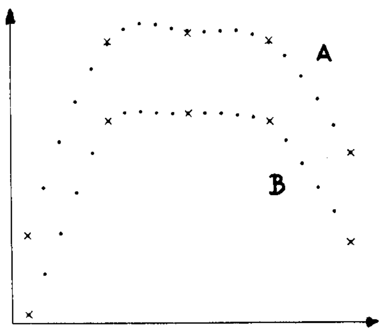

Fig. 2-2 Effect of the automatic weighting during interpolation according to eqn. 2-18
5 given points (x)
21 interpolation points (•)
A without adaption:
bending, smoothing
B with adaption:
bends recognized at the 2nd and 4th point, no smoothing, nearly no bending

3. Surface texture

The surface texture is decisive for the quality of the result. Above all its high frequencies in the form of sharp grey value edges or alternatively changes in the grey value contribute considerably to the precision (cf. Förstner 1985). The long wave parts, the coarse structure, influences the determination of approximate values. Here we went to discuss the special properties of natural and artificial textures with respect to fine and coarse machting.

3.1 Natural textures

By the term natural textures we understand here all surface structures which appear in the image, for which one can make little or no allowance when carrying out the measurement, for example in the case of terrain surfaces or objects which are not accessible. Here one must reckon with two difficulties, namely with reflections or shiny surfaces or surfaces without or with too fine structures.

Only a few materials reflect ideally, i. e. matt. Natural terrain as appearing in photographic scales customary for applications is, therefore, as its reflection qualities is concerned, well suited for correspondence since a pixel receives light from a relatively large area due to the comparatively small scale and because the reflection characteristics, individually possibly unfavourable, compensate one another during the averaging process. The situation is different in close range applications. Here surface shiny to a greater or lesser extent, although locally bounded, can lead to additional grey value changes, which appear either only in one photograph or even in both photographs but which - in relation to the surface- are at non-correspondent points.

Reflections which only appear in one photograph can generally be easily recognized and removed, since no matching is possible. On the other hand reflections in both photographs can generally lead to a highly weighted match due to the contrast, which, however, does not correspond to a surface point but a reflection point (generally behind the surface). This match, a false match from the point of view of the surface, can only be detected during testing for consistency during the surface interpolation, for example with respect to the smoothness of the surface. A detailed analysis of the reflections can nevertheless in the case of a known light source play an important role in a very good reconstruction of the surface (cf. Burkhardt 1985).

Far more awkward are surfaces with insufficient texture, which can occur in all applications. The geometry of the surface can indeed be reconstructed from the shading of an image in case the surface texture is homogeneous. The information derived from the grey values about the surface curvature may also be of value for interpolation. The necessary assumptions, especially about the the reflection behaviour, are generally only approximately true and, therefore, only allow an inexact determination of the form if one does without further back-up information. For surfaces without sufficient texture one has to rely on object edges. They generally appear in the photograph as grey value edges, too. Not only can they be very precisely localized, but they also motivate the linear interpolation between object edge points within the epipolar planes applied in many cases (cf. eg. Ohta/Kanade 1985). Most of the correspondence methods are for this reason based on grey alue edges. The interest operator suggested by Förstner (see Paderes et al 1984) when transferred to epipolar lines also yields edge points, which accordingly are at the same time the points in a grey value profile, at which the matching relatively is most precisely - as was clearly to be expected. Accordingly the evaluation of an existing texture can be based upon accuracy to be expected for matching.

3.2 Surfaces with an artificial texture

For a number of close range applications one is able to specially prepare the possibly reflecting surface for stereo measurement, for example by the spraying-on of colour. Here the question arises which texture is favourable for automatic matching.

Regular structures cannot be considered, on the one hand because they are difficult to produce with curved surfaces, and on the other hand because the regularity can lead to incorrect correspondence. Random patterns as they occur by the spraying-on of colour, are suitable if certain criteria are adhered to, which we want to illustrate here by means of an example.

Let the random pattern consist of black circular discs on a white background, which generally do not overlap, vary in size and are irregular arranged. The sharp contrast provides for a high degree of accuracy for correspondence and, circumstances permitting, makes a processing of binary images possible. The circles are generally represented as ellipses. As stated in paragraph 2.4 one can derive the slope of the surface from the parameters of the ellipse, possibly after averaging several measurements. Three geometric conditions for the size and the distribution of the circles are obvious:

1) In order to be able to recognize and exactly localize the individual circular discs they should have a diameter d of at least 4 pixels: $d \geq 4\,\Delta x$. Hereby it is guaranteed that the circles remain recognizable even with large distortions.

2) In order to be able to separate the circles from one another the space f between the edges should at least be 4 pixels wide: $f \geq 4\,\Delta x$. This requirement together with the following one restricts the size of the circles and prevents too many circles overlapping one another.

3) In order to prevent too large gaps resulting between the circles and in this way in order to be able to record the surface densely enough the distance between the centres of neighbouring circles should not be greater than 16 pixels. One can also make this limit dependent upon the surface curvature. Here we wish to assume $a \leq 16\,\Delta x$.

With a pixel size for example of 0.02 mm and $d + a = f$ there results for the diameter of the circular discs a range of

$$4\,\Delta x \leq d \leq 12\,\Delta x \quad \text{or} \quad 0.08\text{ mm} \leq d < 0.24\text{ mm} \tag{3-1}$$

and for the distance between the circle centres a range of

$$8\,\Delta x \leq a \leq 16\,\Delta x \quad \text{or} \quad 0.16\text{ mm} \leq a \;\; 0.32\text{ mm} \tag{3-2}$$

With an average distance $\bar{a}$ of the circles from one another of $\bar{a} = 12\,\Delta x = 0.24$ mm there are approximately 20 circles in a mm², which cover approximately 40 % of the surface. With a photograph scale of 1 : 20 (distance to object: 2 m) there are under these circumstances approximately 5 circles in a cm². Fig. 3-1 illustrates an example. It resulted from a random choice of 20 centres and the related diameters between 4 and 12 Δx . The smallest distance was not directly taken into consideration. The average distance does, however, lie roughly within the above-mentioned range. Analogously other random patterns can be produced and adapted to the individual task at hand.

Fig. 3-1 Random pattern with circular discs, Surface: 1 mm² or 50 x 50 pixels

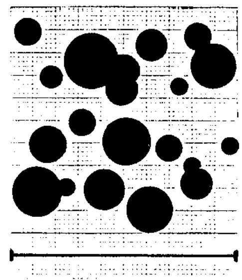

3.3 Surface with a projected texture

Specially projected structures are a well-known aid to enable the measurement of surfaces which are poor in texture. One can distinguish here two ways of taking of the photograph:

1) One of the two sensors is replaced by a projector, which contains the pattern in the image plane. In this case it is enough to take only one photograph from another visual angle in order to be able to carry out a stereo measurement. Matching consists in finding the features contained in the projected image. In order to obtain a geometrically precise measurement it is necessary to measure the mask and to calibrate the projector.

2) The second possibility consists in staying with a stereo photograph and in projecting a pattern onto the surface from a third location - somewhere between the sensors. In principle nothing changes with automatic measurement since the natural texture is replaced by an artificial one. In contrast, however, to the first situation the geoemtric calibration of the mask and of projector is not necessary.

Since a calibration of the cameras is necessary anyway for precision measurements and since this is also carried out using standard methods the second situation is preferable to the first.

The measurement, in particular the correspondence, can be cosiderable simplified by the choice of a favourable mask. The frequently used grid or line rasters are suitable for a precise correspondence due to their fine structure. They do, however, present difficulties for a coarse correspondence because of their rigorous regularity.

The following requirements have to be met by a projected mask in order to make automatic correspondence as simple as possible:

a) Because of the assumed knowledge about the epipolar geometry a line pattern at right angles to the base is sufficient. The position on the lines is determined by the epipolar line.

   A mask with straight lines allows the recording of all jumps in the surface. The lateral slope of the area can be directly derived from the differences in slope of the projected lines. If the lines are the same distance apart from one another, or if the distances are known, one can also determine the local longitudinal slope of the surface. In order to avoid a calibration of the pattern line maks with random distances are not taken into consideration. Since lines of random direction are easy to recognize in the image surfaces of any given slope can - at least theoretically - be measured.

Photogrammetrische Woche 1985
Institut für Photogrammetrie
Schriftenreihe, Heft 11, 1986

b) All lines should be numbered.
In this way a clear correspondence is possible. The searching for a particular line takes place by direct access, possible in 2 or 3 stages. The search area is not restricted to the visual field of digital camera or alternatively to each of the observed possible small windows. Occlusions do not lead to identification errors as possibly the case with patterns, where only every tenth line is numbered. Several images can be treated one after another.

c) The numbering should be clearly legible for both the computer and the operator. In this way a rapid decoding by the computer is possible and also - with analytical plotters - a transition to manual measurement.

d) The numbering should require as little space as possible and should as regards its structure assist the stereo measurement. The image window necessary for the recognition of the line is thus kept small.

e) The lines should not be further apart from one another than 16 or 20 pixels (see circular pattern). In this way it is guaranteed that a suffiency dense recording of the surface is possible even for highly curved areas of the surface.

f) The space between the lines should be at least 4 pixels wide (see above). An identification of the lines is thus possible even if there is a sharp longitudinal slope or if local exposure effects are present.

g) The pattern should to a certain extent enable the recognition of the natural surface texture.

For this reason only a black and white texture can come into question. The mask then also allows a local adjustment of the line detectors. A detailed radiometric calibration of the digital camera thus becomes superflous.

The masks in Fig. 3-2 fulfill all the named requirements. They consist of two components: the measurement lines, which have a regular structure and the coded numbers which vertically repeat themselves and which are equally suited for the purpose of measurement. The patterns represent the lines 80 to 92. The numbers are binary coded, whereby the consecutive number of the bits, counting from right to left, is also represented in the figure: e, g, $89_{10} = 1011001_2$. The last bit (the 9th in 3-2a and the 8th in 3-2b) serve in each case as a control bit (parity check). An even number of bits was assumed here as the last bit is set as e. g. $91_{10} = 1011011_2$. The pattern in Fig. 3-2a contains the line numbers in the narrowest space, on the other side the distance between the measurement lines in Fig. 3-2b, therefore, is smaller. When identifying the number of a line the computer can rely on the measurement lines and can very accurately predict from their geometrical arrangement the positions at which the coding of the lines (in this case left of the lines) is placed. In this way the suspectability to disturbance is greatly reduced, since no positioning is involved in the decoding. Should a number be not decodable due to disturbances or occlusions one can find a usually readable number in the vicinity within a small image window. Thus the selection of only a small sensor section is necessary for the recognition of the momentary position on the surface. The horizontal lines primarily serve the purpose of determing the position of the coded numbers. They can, however, also be advantageous of the measurement if the mask is projected diagonal ($\pm 20°$) to the base.

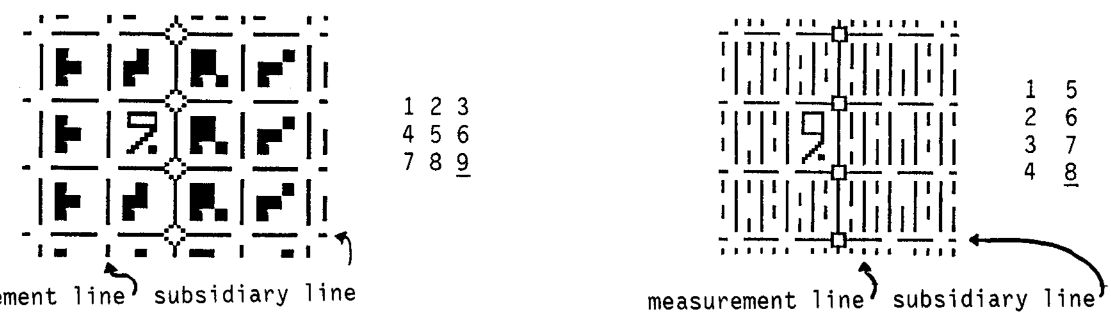

Fig. 3-2 artificial patterns for projection
measurement lines numbered, left of the line, binarily coded, parity bit underlined
10th line (9. $\hat{=}$ 90) marked
distance of the measurement lines: a) 16 pixels b) 16 pixels for counting lines
8 pixels for subsidiary lines
size of the bits: a) 9 pixels b) 4 pixels
word length: a) 8 bits b) 7 bits

The distances and the breadth of the measurement lines as well as the size of the coding are individually variable; similar patterns as in Fig. 3-2, which show the same advantages, are thus conceivable. In particular, the numbering area can be enlargened by changing the word length. A coding of the vertical coodinates is also possible.

Altogether means are available for projection with coded patterns, which are easily produced with a precision drawing table. They remove a large number of the difficulties, which occur with natural patterns. Above all the searching for given positions and the treatment of any given slopes of the surface are made considerably easier.

4. Representation of the surface by measurement elements

4.1 Criteria for the selection of surface features

As image matching the recording of surfaces in the conventional sense consists of two stages (cf. Makarovic 1984): the extraction of features of the surface and the determination of the exact position on the surface. Only in the case of complex surfaces, however, are the two steps carried out separately.

The precision of the digital surface model is determined to a large extend by the distribution of the measurement positions. The quality of the measurement is determined not so much by the precision as by its ability to represent the surface; the interpolation method is only of secondary importance (see Ackermann 1980). The recording of surfaces by means of measurement points and measurement lines, in particular break lines, has been intensively examined in the last few years. On the one hand the investigations concentrated on optimal point density (cf. Tempfli 1982), the automatic adaptation of the point density to the surface form (Progressive Sampling, Makarovic 1973) and on the other hand the adaptive recording of the surface information, which is connected with line information (Composite Sampling, Makarovic 1984). All investigations are based on the ability of the operator to interprete the surface form before the actual measurement or rely on the information on the surface, derived from a coarse grid measurement, as progressive sampling. The situation regarding surface measurement presents itself anew with automatic stereo, namely for two reasons:

a) the stereo model which is available to the operator for feature extraction is not yet available for the computer for this task.

b) the hitherto existing programmes for the interpretation of individual photographs are not by a long way developed to such an extent that the extraction of surface features can attain a sufficiently satisfactory quality under not too restricted conditions.

In principle there thus exist three alternatives for the extraction of surface features:

1) The measurement elements are selected, placed and coded according to the surface for, as in terrestrial surveying (incl. break lines), structure lines (spot heights).

2) The measured points are arranged in a grid and circumstances permitting are locally condensed in grid form (progressive sampling).

3) The position of the measuring elements are derived from the interpretation of a single image.

Manual measurement can follow all three strategies. The feature extraction, depending upon the surface form, is not possible with automatic measurement (see above). The second alternative has certain disadvantages. As with every other grid-related selection method the point selection according to the method of progressive sampling presents difficulties when the points fall on areas of poor texture or on objects which do not represent the surface (e. g. trees, houses, ditches etc.). The reaction of the operator namely to select and measure a point in the vicinity suitable for stereo measurement can be copied on the computer as long as it can be guaranteed that the point, found possible by an interest operator, really does represent the surface. Since this has in any case to be tested by measuring further surrounding points one can no longer talk of a raster measurement. A rudimentary singly image interpretation is actually carried out because interest operators usually search for very simple characteristics, possibly points with pronounced grey level transitions. With automatic systems the measurement points will, therefore - at least for the time being - be restricted to points which are recognizable in one image and which are suitable for correspondence. The system measures where it expects to be able to carry out a measurement.

The areas between the measurement spots which are either without texture or poor in texture point to the fact that the surface is very smooth, in the sense of slightly curved, so that a simple interpolation is not only allowed but justified. All non-photogrammetric automatic methods for surface measurement are based on these facts (cf. examples 1 and 2, pgh. 5).

4.2 Characteristics for surface measurement

There exist a number of image features for the purpose of correspondence, of which one expects that they represent essential surface features. Grey value edges are the most wide-spread for correspondence. They can easily be extracted - as long as they do not have to serve as a basis for an interpretation, and they are to a large extent invariant against geomeric and radiometric changes (cf. Grimson 1981, Ohta/ Kanade 1984, Baker 1983, Smith/Wolf 1984).

In order to diminish the number of possible correspondence, image segments derived from edges are sued for correspondence. The theoretically higher reliability is obtaiend at the cost of a greater complexity of the correspondence algorithm, which is justified by the suspectability of the segmentation to small disturbances. On the other hand topographic characteristics of the grey value function, such as high and low points, that is light or dark points, or ridge and valley lines, that is light or dark lines in the image, seem to be well suited for correspondence, since they are in particular invariable against monotone transformations of the grey values (cf. Haralick et al. 1980, Zimmermann/kories 1984).

5. Examples for surface measurement from image pairs

Three examples are to represent the efficiency and the diversity of the solutions of surface measurement.

Example 1:

The investigations for understanding the human visual system at the MIT aim at a computer simulation of stereopsy. The underlying model was developed by Marr and Poggio and realised and worked out by Grimson (1981, 1984). The system for surface measurement which thus originated is able to handle highly different object forms and surface textures.

Fig. 5-1 shows a random stereogram and the digital surface model derived from it.
The correspondence algorithm is based on grey value edges, which are - in total four - band-pass filtered images with varying degrees of smoothness. Two of these are shown in Fig. 5-2. The correspondence takes place hierachically, beginning with the edges of the most highly smoothed image. As one can clearly see neither the human visual system nor this algorithm needs clues from the single image in order to obtain a stereo impression. Fig. 5-3 shows that this same method can also successfully handle aerial photographs.

Example 2:

The method of Ohta and Kanade (1985) is similarly based on grey value edges. The photographs are, however, hardly smoothed. The correspondence algorithm uses methods of dynamic programming and works at one level. The correspondence algorithm uses not only the consistency condition within the epipolar lines but also the compatability of the solution between the lines, as it occurs at edges across the epipolar lines. In this way the percentage of incorrect correspondence is lessened by one order.

Fig. 5-4a shows an aerial photograph pair of the Pentagon, Fig. 5-4b all the extracted edge points within the epipolar lines and the related grey value edges derived from them (Fig. 5-4c). The result is represented in Fig. 5-4d. It shows that the method is able to stereoscopically measure buildings. The walls which in reality are perpendicular appear slanting in the figure. since only a linear interpolation takes place between the correspondent edges within the epipolar lines.

Example 3:

The last example is to show that an accuracy is obtainable with correspondence algorithms, which is usfficient for some applications where precision is not of the highest priority. A photograph of a specially prepared surface of a carbody was stereoscopically taken at photo scale 1 : 20. A section was firstly measured manually, secondly with least squares matching (cf. Pertl 1985) and also with a feature based matching procedure (Förstner 1985). The points selected by this correspondence algorithm are shown in Fig. 5-5a. The surface model derived from this is represented in Fig. 5-5b.An editing of the data was not necessary. The comparison with the manual measurement (Fig. 5-5c) shows that the main structure was correctly recorded. The histogram of the differences in altitude between manual and automatic measurement demonstrates a systematic error of - 0.4 mm. The standard deviation of 0.6 mm at the object corresponds to a measurement accuracy of approximately 10 µmm, or with a pixel size of 40 µm, to a standard deviation of a 1/4 pixel size. This error is approximately as large as the rounding errors of the of the coordinating of the selected points.

The examples clearly show that the automatic methods for surface measurement have reached a point which bears the promise of practical application in the near future. The representation of the digital surface model is, however, only the first step towards automatic interpretation of the data, possibly for the video-steering of machines or automatic mapping.

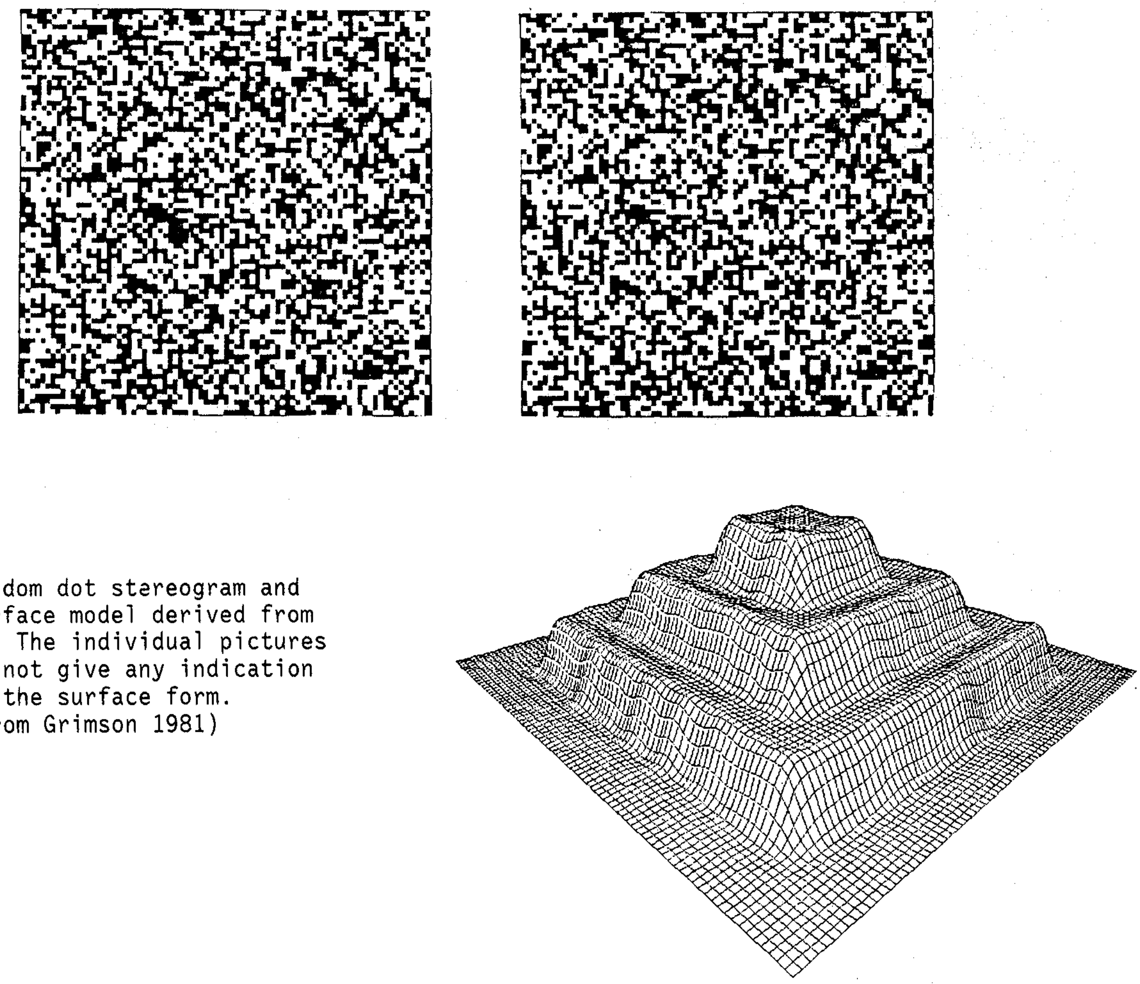

Fig. 5-1 Random dot stereogram and surface model derived from it. The individual pictures do not give any indication of the surface form. (from Grimson 1981)

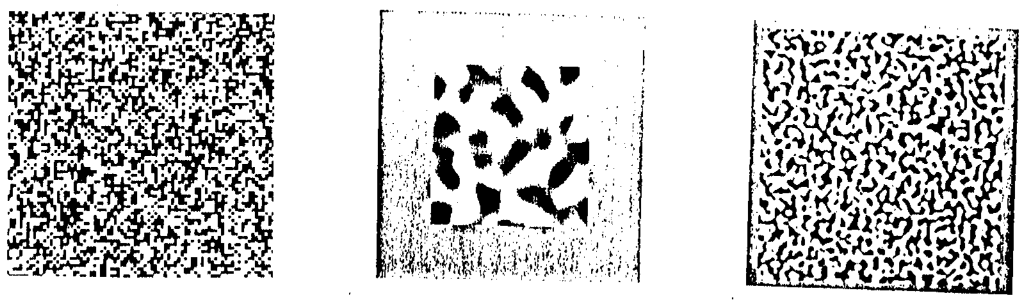

a. b. c.

Fig. 5-2 Extraction of characteristics according to Grimson (1981)
a) random dot image
b) highly smoothed image (band pass)
c) slightly smoothed image (band pass)
d) edges of b.
e) edges of c.

The edges are selected per epipolar line, the sign of the changes in grey value and the direction of the edge are used for the preliminary correspondence.

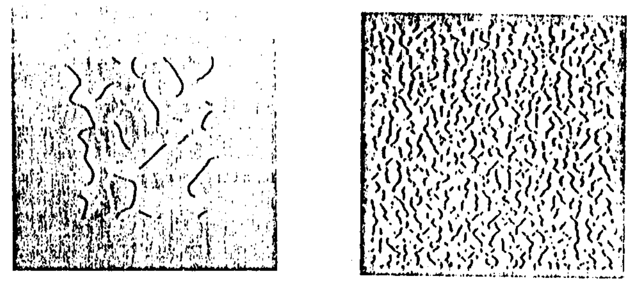

d. e.

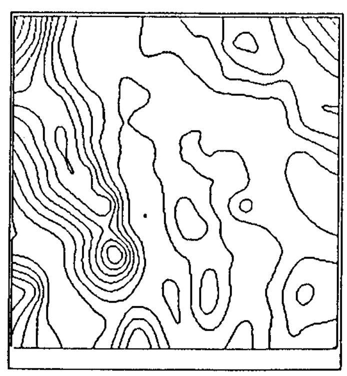

Fig. 5-3 Pair of aerial photographs, area of Phoenix, and the contour lines derived from them (from Grimson 1984)

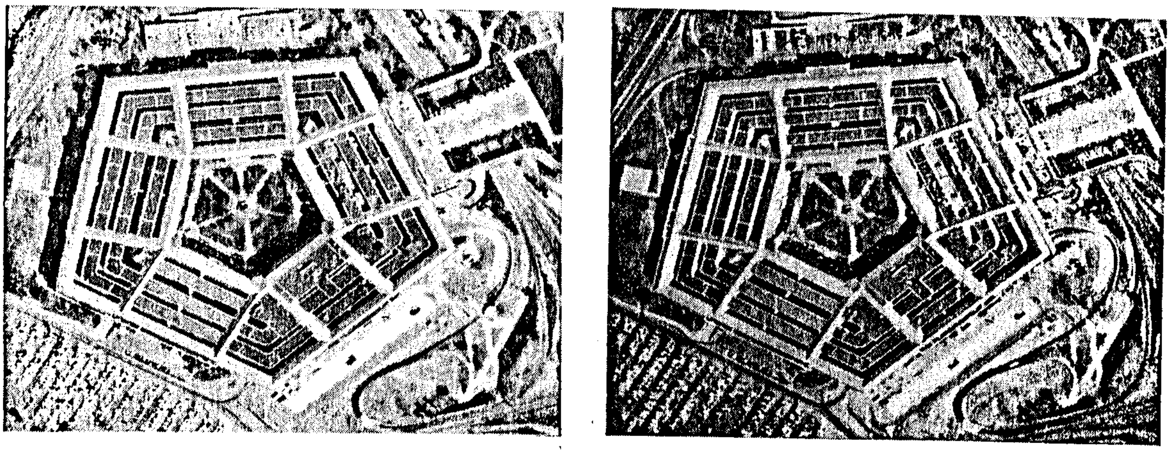

a.

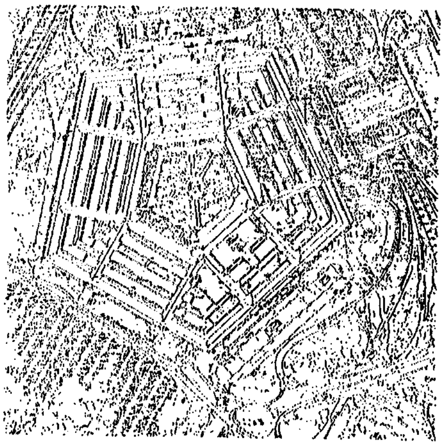

b.

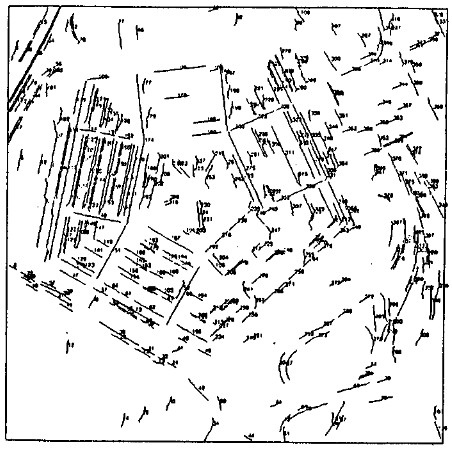

c.

Fig. 5-4 a. stereo pair
b. edge points extracted within the epipolar lines
c. connected edges derived from b.
d. digital surface model (from Ohta/Kanade 1985)

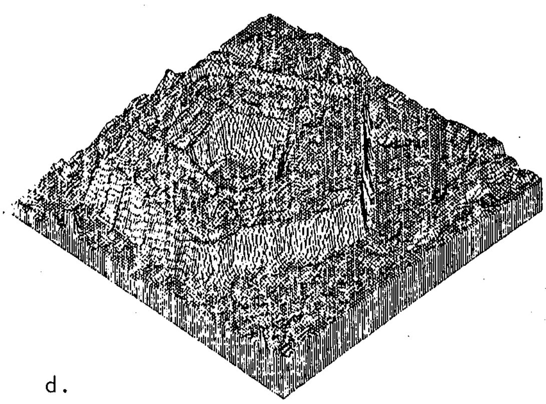

d.

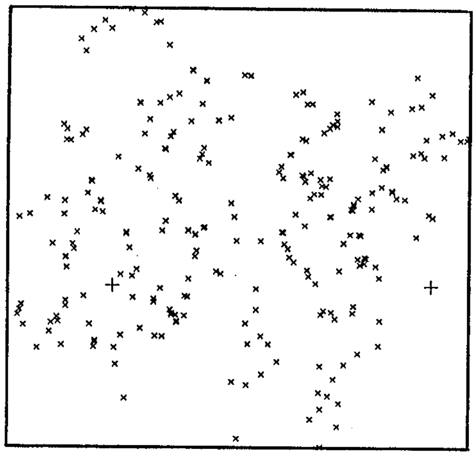

a.

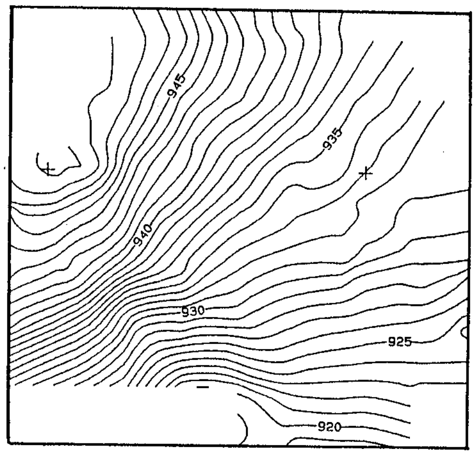

b.

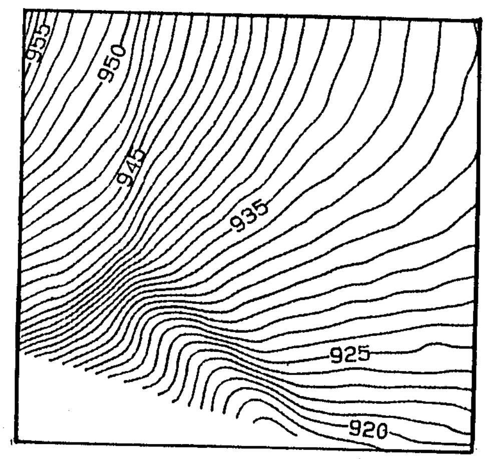

c.

Fig. 5-5 Comparison of manual and automatic surface measurement photograph scale 1 : 20
a. selected and corresponded points (Förstner 1985)
b. contour lines derived from a. distance 1 mm
c. result of manual measurement
d. histogram of the attitude differences of b. and c.
systematic error - 0.4 mm
mean difference 0.6 mm
≙ 10 µm ≙ 1/4 pixel

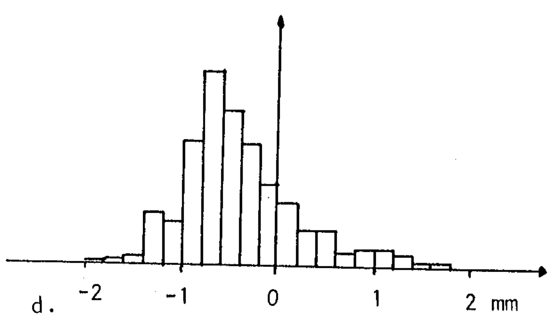

d.

Literature

Ackermann F. (1980): The Accuracy of Digital Height Models, Schr. d. Inst. f. Photogr. Stgt., Heft 6, S. 133-144

Baker H. H. (1982): Stereo Vision Systems, IEEE Proc. of the Int. Conf. on Cybernetics and Society, Seattle, 1982, pp. 322-326

Baker H. H. (1983): Surfaces from Mono and Stereo Images, Specialist Workshop on Pattern Recognition in Photogrammetry, Graz, 1983

Ballard D. H., Brown C. M. (1982): Computer Vision, Prentice Hall, NJ, 1982

Barnard S. T., Fischler M. A.(1982): Computational Stereo, Comp. Surveys 14, 1982, 553-572

Binford T. O. (19881): Inferring Surfaces from Images, in Brady (1981), pp. 205-244

Brady J. M. (1981, ed.): Computer Vision, North Holland, 1981; Reprint from AI 17, 1981

Burkhardt R. (1985): Die Spiegeloptische Formbestimmung der Augenoberfläche (Cornea-Photogrammetrie), Bildmessung und Luftbildwesen 5/85, S. 152-162

Case J. B. (1981): Automation in Photogrammetry, Photogr. Eng. 47, 1981, pp. 335-341

Ebner H. (1979): Zwei neue Interpolationsverfahren und Beispiele für ihre Anwendung, Bildm. u. Luftbildw., 1979, S. 15-27

Förstner W. (1983): On the Morphological Quality of Digital Elevation Models, ISPRS WG III/1 Int. Coll. on Math. Aspects of DEMs, Stockholm 1983, pp. 6:1-6:18

Förstner W. (1985): Prinzip und Leistungsfähigkeit der Korrelation und Zuordnung von Bildern, Phot. Woche 1985

Grimson W. E. L. (1981): From Images to Surfaces: A Computational Study on the Human Early Visual System, MIT-Press, 1981

Grimson W. E. L. (1984): Computational Experiments with a Feature Based Stereo Algorithm, IEEE Trans. on Pattern Analysis and Machine Intelligence, PAMI-7, 1985, pp. 17-34

Gülch E. (1985): Instrumentelle Realisierung und Kalibrierung der digitalen Bildkorrelation am Planicomp C 100, Photogr. Woche 1985

Haralick R. M. (1980): Using Perspective Transformations in Scene Analysis, Comp. Graph. and Image Proc., 13, 1980, pp. 191-221

Haralick R. M., Watson L. T., Laffey T. J. (1983): The Topographic Primal Sketch, The Int. J. of Robotics Research, 2-1, 1983, pp. 50-72

Helava U. V., Chapelle W. E. (1972): Epipolar Scan Correlation, Bendix Techn. J., 5, 1972, pp. 19-23

Hobrough G. (1978): Digital On-Line Correlation, Symp. üb. den Einsatz digit. Kompon. in der Photogrammetrie, Inst. f. Photogr. u. Ing.-verm., Univ. Hannover, Heft 2, 1978

Ikeuchi K., Horn B. K. P. (1981): Numerical Shape from Shading and Occluding Boudaries, in Brady (1981), pp. 141-184

Konecny G., Pape D. (1981): Correlation Techniques and Devices, Phot. Eng. 47, 1981, pp. 323-333

Kories R. R. (1985): Bildzuordnungsverfahren für die Auswertung von Bildfolgen, Photogr. Woche 1985

Kreiling W. (1978): Off-Line Correlation in General Purpose Computers, Symp. ü. den Einsatz digitaler Kompon. in der Photogr., Inst. f. Photogr. u. Ing.-Verm., Hannover, Heft 2 1978

Li D. (1983): Ein Verfahren zur Aufdeckung grober Fehler mit Hilfe der a posteriori Varianzschätzung, Bildm. u. Luftbildw., 5, 1983

Makarovic B. (1973): Progressive Sampling for Digital Terrain Models, ITC Journal, 1973-3, pp. 397-416

Makarovic B. (1979): Composite Sampling for Digital Terrain Models, ITC Journal, 1979

Makarovic B. (1984): Structures for Geo-Information and their Application in Selective Sampling for Digital Terrain Models, ITC Journal, 1984, pp. 285-295

Nagel H. H., Enkelmann W.(1984): Berechnung von Verschiebungsvektoren in Bildbereichen mit linienhaften oder partiell homogenen Grauwertverteilungen, Inf. Fachb., 87, Springer, 1984 pp. 154-161

Ohta Y., Kanade T. (1985): Stereo by Intra- and Inter-Scanline Search Using Dynamic Programming, IEEE Tr. on Patt. Analysis and Mach. Intell., PAMI-7, 1985, pp. 139-154

Paderes F. C., Mikhail E. M., Förstner W. (1984): Rectification of Single and Multiple Frames of Sattelite Scanner Imagery Using Points and Edges as Control, NASA-Symp. on Math. Patt. Recognition and Image Analysis, Houston

Smith G. B., Wolf H. C. (1984): Image-to-Image Correspondence: Linear-Sructure Matching, NASA-Symp. on Math. Patt. Recogn. and Image Analysis, Houston, 1984

Pertl A. (1985): Empirische Ergebnisse der automatischen Parallaxen- und Punktmessung, Photogr. Woche 1985

Schwidefsky K., Ackermann F. (1976): Photogrammetrie, Teubner, Stuttgart, 1976

Tempfli K. (1982): Genauigkeitsschätzung digitaler Höhenmodelle mittels Spektralanalyse, Geowiss. Mitt., 22, 1982

Wiesel J. (1981): Paßpunktbestimmung und geometrische Genauigkeit bei der relativen Entzerrung von Abtastdaten, DGK, C 268, München

Woodham R. J. (1980): Photometric Method for Determining Surface Orientations from Multiple Images, Opt. Eng., 19, 1980, pp. 139-144

Woodham R. J. (1981): Analysing Images of Curved Surfaces, in Brady (1981), pp. 117-140

Wrobel B. (1981): Über die heutigen Anwendungschancen der Nahbereichsphotogrammetrie, Wiss. Arb. der Fachr. Verm.-wes. der Univ. Hannover, Heft 100, 1981, S. 201-220

Zimmermann G., Kories R.R. (1984): Eine Familie von Bildmerkmalen für die Bewegungsbestimmung in Bildfolgen, Inf. Fachb., 87, Springer, 1984, S. 147-153

Photogrammetrische Woche 1985
Institut für Photogrammetrie
Schriftenreihe, Heft 11, 1986

Abstract

One of the most important features for describing an object is the geometric form of its surface. The paper discusses aspects which are specific for the automatic mensuration of surfaces from stereo images. Specifically these are the geometry of the design in relation to the surface, the evaluation and choice of surface textures and the representation of the surface by measuring elements. Three examples demonstrate the efficiency and versatility of existing solutions for automatic surface determination.

AUTOMATISCHE ERFASSUNG VON DIGITALEN OBERFLÄCHENMODELLEN

Zusammenfassung

Eines der wichtigsten Merkmale zur Beschreibung eines Objektes ist die geometrische Form seiner Oberfläche. Der vorliegende Beitrag behandelt für die automatische Oberflächenmessung aus Bildern spezifische Aspekte, insbesondere die Geometrie der Aufnahme und der Oberfläche, die Beurteilung oder Auswahl von Oberflächentexturen und die Repräsentation der Oberfläche durch Meßelemente. Drei Beispiele stellen die Leistungsfähigkeit und die Verschiedenartigkeit vorhandener Lösungen dar.

Dr.-Ing. Wolfgang Förstner
Institut für Photogrammetrie
Universität Stuttgart
Keplerstr. 11
D-7000 Stuttgart 1